September 22, 2008

Title: Spatial Distribution of Neurons in the Dorsal Lateral Geniculate Complex of Freshwater Turtles

Authors: John Curtis[1] & Philip S. Ulinski

Addresses: Department of Organismal Biology and Anatomy, The University Chicago, Chicago, IL 60637

Abstract

The spatial distribution of neurons in the turtle's dorsal lateral geniculate nucleus was quantified for three turtle brains and then compared to the distribution of retinal ganglion cells in order to estimate the overall convergence of ganglion cells to geniculate neurons, and also to estimate how this convergence varies regionally in the turtle's visual field. The results show that turtles have 10,000 to 20,000 geniculate neurons, which vary in density from 10,000 to 60,000 cells/mm^2. Each of the three geniculate nuclei examined display two areas of peak cell density one located in the ventral-rostral region of the geniculate and another located in the central-rostral region of the geniculate. The overall convergence of ganglion cells to geniculate neurons is 27:1. The convergence appears to be highest in the turtle's central visual field and lower in the peripheral visual field.

Key Words: dorsal lateral geniculate complex, turtles, spatial distribution, convergence ratio, coverage factor.

Introduction

Turtles have a dorsal lateral geniculate complex that receives direct projections from retinal ganglion cells (Hall & Ebner, 1970; Rainey & Ulinski, 1986; Review: Ulinski, 1999) and projects, in turn, to a visual cortex (Hall & Ebner, 1970; Hall et al. 1977; Belekhova et al., 1979; Ouimet et al., 1985, Rainey & Ulinski, 1986; Review: Ulinski, 1999). The freshwater turtle, *Pseudemys scripta*, has approximately 364,500 ganglion cells distributed inhomogeneously over the retinal surface (Peterson & Ulinski, 1979). They occur with greatest density in a visual streak situated along the naso-temporal axis of the retina. An area of peak ganglion cell density is embedded in the visual streak. Ganglion cells fall into three classes based on soma size (Peterson & Ulinski, 1979) and

axonal conduction velocity (Woodbury & Ulinski, 1986). The numerically smallest group are large, displaced ganglion cells that project to the accessory optic system ( ). Ganglion cells with intermediate and large soma sizes have intermediate and slow axonal conduction velocities ( ) and apparently project to both the optic tectum and dorsal lateral geniculate complex via axons that bifurcate in the optic tract ( ). There is no agreement on the number of physiological classes of ganglion cells present in turtles (reviews: Peterson, ; Granda,), but it is clear that a relatively large fraction of turtle ganglion cells have complex receptive field properties and show distinct direction and speed tuning ( ).

The dorsal lateral geniculate complex in turtles is a crescent-shaped structure situated immediately internal to the optic tract (Rainey & Ulinski, 1986). It contains two morphologically distinct groups of neurons, cell plate cells and neuropile cells, arranged so that the complex has a laminar organization. In contrast to the geniculate layers seen in many orders of mammals, the majority of neurons are not confined to a specific lamina. The somata of cell plate cells are densely packed along the inner face of the complex to constitute a cell plate layer (Rainey & Ulinski, 1986). Their dendrites extend toward the optic tract to form a neuropile layer. The proximal shafts of the dendrites are thick and lack dendritic specializations, but their distal dendrites branch into finger-like arborizations that form reciprocal dendrodendritic contacts with neighboring cell plate cells. Neuropile cells have their somata scattered within the neuropile layer, relatively near the optic tract, and dendrites that extend parallel to the optic tract. There are clear spatial variations in the size and density of neurons in the cell plate and neuropile layers of the geniculate complex and in the sizes of the dendritic arbors of the cell plate cells (Rainey & Ulinski, 1986). The complex can be

divided into three subnuclei (the dorsal subnucleus, the ventral subnucleus and subnucleus ovalis) based on these variations in cell density and morphology. The retinogeniculate projection is organized so that the nasotemporal axis of the retina is mapped along the rostrocaudal axis of the geniculate (Figure 1), and the dorsoventral axis of the retina is mapped along the dorsoventral axis of the geniculate (Ulinski & Nautiyal, 1988). The majority of ganglion cells project to the contralateral geniculate, but there is a small projection from the ventral rim of the ipsilateral retina to a ventral strip of the geniculate, which receives binocular inputs (Figure 1). Retinogeniculate axon terminals form three morphologically distinct groups that end preferentially in specific laminae in the geniculate complex (Sjöström & Ulinski, 1985). Terminals originating from thin caliber axons form small terminals with clear, round synaptic vesicles that are presynaptic to the finger-like terminal arbors of the cell plate cells and, presumably, the neuropile cells (Ulinski, 1986). Terminals originating from thick caliber axons form large terminals with clear, round synaptic vesicles that are presynaptic to the proximal shafts of cell plate cells. It appears, then, that different groups of ganglion cells terminate upon different segments of the dendrites of cell plate cells. This implies that turtle geniculate neurons, in contrast to the pattern typical in mammals, receive convergent inputs from different functional classes of ganglion cells. The cell plate cells project to the ipsilateral visual cortex ( ). Whether or not the neuropile cells project to the cortex is controversial ( ).

Place Figure 1 here

The first part of this paper characterizes the numbers and spatial distribution of

neurons within the geniculate complex of freshwater turtles. The quantitative analysis confirms the qualitative description of Rainey & Ulinski (1986) and demonstrates a marked variation in the spatial distribution of neurons within the geniculate complex. The second part of the paper determines the relationship between the number of ganglion cells and geniculate neurons. It then characterizes the spatial distributions of ganglion cells and geniculate neurons by estimating coverage factors and convergence ratios for different points in the retinogeniculate projection. Coverage factors for geniculate neurons are large, and that there is a greater convergence of ganglion cells to geniculate neurons than has been reported for the retinogeniculate projection in mammals. These findings suggest that there are fundamental differences in the functional organization of the geniculocortical pathway between turtles and mammals.

Materials and Methods

Brains from three turtles of the genera *Pseudemys* or *Chrysemys* were used. Turtles were perfused intracardially with 0.9 % saline, followed by 10 % formaldehyde. One brain was embedded in paraffin and sectioned in the coronal plane at 15 μm. Two brains were embedded in celloidin and sectioned in the transverse plane at 25 μm. All sections were stained for Nissl substance with cresyl violet.

Drawings of all of the geniculate neurons in each section through each brain were produced using a *camera lucida* at an overall magnification of 390 X (Figure 1). The cytoarchitectonic description of the geniculate complex by Rainey & Ulinski (1986) was

used to determine the borders of the geniculate complex and its subdivisions. Neurons were easily distinguished from non-neuronal cells on the basis of their size and morphology. Neurons were larger than glial cells and morphologically distinct from endothelial cells. Only neurons with discernable nuclei were drawn. Each geniculate section was systematically divided along its dorsalventral axis into several rectangular areas. Each area was 50 μm high, but individual areas varied in their medial-lateral dimensions depending on their positions in the geniculate. Since sections were 15 μm – 25 μm thick, each area represented a rectangular solid of the geniculate complex. Cell plate and neuropile cells within each rectangular solid were counted and used to prepare maps of the density of cell plate cells, neuropile cells and total geniculate neurons as a function of rostrocaudal and dorsoventral position on the surface of the geniculate. Neuronal counts were corrected for double counting of neurons split into two neighboring sections using the Abercrombie (1946) correction factor

$$\frac{N_i}{n_i} = \frac{t}{t+d}$$

where N_i is the corrected number of neurons in section i, n_i is the number of neurons counted in the section, t is the measured section thickness in microns and d is the diameter of the neuronal nuclei in microns.

Results

Total Number of Geniculate Neurons

The total number of neurons in the geniculate complex, and the number of cell plate and neuropile cells, was counted and corrected for double counting in each of the three geniculate complexes (Table 1). The mean $\pm$ SEM number of total cells was 13,384 $\pm$ 4,155. The mean $\pm$ SEM number of cell plate cells was 12,273 $\pm$ 3,935. The mean $\pm$ SEM number of neuropile cells was 1,111 $\pm$ 227. Cell plate cells, thus, constitute 92 % of the cells in the geniculate complex. Neuropile cells constitute 8 % of the cells in the geniculate complex.

Place Table 1 here

Spatial Distribution of Geniculate Neurons

Figures 2, 3 and 4 are isodensity maps for the three geniculate complexes. They are contour plots of the density of geniculate neurons, projected onto the external face of the geniculate complex, as a function of position in the geniculate complex. Each figure shows separate plots for all geniculate neurons (top), cell plate cells (middle) and neuropile cells (bottom). The three sets of isodensity maps are similar and confirmed the finding (Rainey & Ulinski, 1986) that there are significant variations in the density of geniculate neurons along the rostrocaudal and dorsoventral axes of the geniculate.

The density of all geniculate neurons varies from a minimal value of about 10,000 cells/mm^2 to a maximal value of 48,000 – 60,000 cells/mm^2. Cell density in each case increases from caudal to rostral along the rostrocaudal axis. There are two peak density areas. The major peak is positioned ventrally near the midpoint of the rostrocaudal axis. The second minor peak is positioned dorsally near the rostral pole of the

geniculate. The spatial distribution of cell plate cells closely resembles the distribution of all of the cells. This is expected because cell plate cells are the vast majority of cells in the geniculate complex. By contrast, the density of neuropile cells shows relatively little variation along either the rostrocaudal or dorsoventral axes of the geniculate, and does not show distinct peaks.

Place Figures 2, 3, and 4 here

Details of the spatial distribution of all geniculate neurons are shown in Figures 5 and 6, which are plots of cell density for all geniculate neurons along representative horizontal (Fig. 5) and vertical (Fig. 6) transects through the geniculate complex from the brain sectioned at 15 μm (Geniculate–2). This brain is used for illustration because the thinner sections provide a greater number of data points. Horizontal transects are not strictly horizontal. Rather, they follow the general curvature of the geniculate complex. Three horizontal transects (B, C and D) show the location of the two high density areas. They are clearest in transect C, where they occur at 260 μm and 620 μm from the rostral pole of the geniculate, and in transect D, where they occur at 250 μm and 540 μm from the rostral pole. The horizontal transects also show that the density of cells is highest in the rostral half of the geniculate. Vertical transects were taken orthogonal to the horizontal transects. Transects C and D pass through the major peak density area. Transect B passes through the minor peak density area. Transects through the peak density areas characteristically show that the cell density decreases rapidly along the ventral slope of the peaks. Transects A and F pass through the rostral and caudal poles of the complex, respectively, and show that the cell density is distributed symmetrically around a gentle peak.

Place Figures 5 and 6 here

Coverage Factors

In addition to systematic variations in the density of geniculate neurons throughout the geniculate complex, Rainey & Ulinski (1986) found variations in the sizes of dendritic fields of neurons in geniculate complex. Cell density and dendritic field size can be interrelated using the concept of a coverage factor (Review: Rodieck, 1998), which is a measure of the degree of overlap between neighboring cells. A coverage factor of 1.0 indicates that a surface (such as the retina or geniculate face) is evenly tiled with dendritic fields that do not overlap. Coverage factors greater that 1.0 indicate overlapping dendritic fields. Coverage factors for each geniculate subnucleus were calculated by multiplying the minimum and maximum cell densities in each subnucleus by the average dendritic field area for each subnucleus (Table 2). Dendritic field areas were calculated by estimating the major and minor dendritic field diameters of cells in sagittal sections, using data from Rainey & Ulinski, (1986). It was assumed that dendritic fields form ellipses when projected onto the external face of the complex. Dendritic field areas were largest in the ventral subnucleus, smallest in the dorsal subnucleus, and intermediate in size in the subnucleus ovalis. Specifically, cell plate cells in subnucleus ovalis have dendritic fields ranging from 0.042 to 0.091 mm^2, cell plate cells in the dorsal subnucleus have dendritic fields ranging from 0.006 to 0.156 mm^2, and cell plate cells in the ventral subnucleus have dendritic fields ranging from 0.180 to 0.262 mm^2. Overall, the coverage factors were high and varied from a minimum of 215 to a maximum of 6,810. The dorsal subnucleus had the smallest

coverage factors, ranging from 215 to 2,064. Coverage factors for subnucleus ovalis were two to three times greater than for the dorsal subnucleus, ranging from 469 to 4,288. Coverage factors for the ventral subnucleus were three to four times greater than the dorsal subnucleus, ranging from 1,135 to 6,810.

Place Table 2 here

Convergence Ratios

Large values for coverage factors raise the possibility that many individual retinal ganglion cells converge upon an individual geniculate neuron. An overall convergence ratio of ganglion cells to geniculate neurons can be obtained by dividing the average number of ganglion cells by the average number of geniculate neurons. Peterson & Ulinski report a mean of 364,500 retinal ganglion cells in *Pseudemys* retinas. Using our mean of 13,484 neurons in the geniculate complex gives a mean convergence ratio of 27:1.

However, the spatial variations in the densities of both ganglion cells and geniculate neurons make it likely there are also spatial variations in the convergence ratio. Plots showing the spatial variation in convergence ratios were constructed in three steps. The first step was to express the densities of ganglion cells and geniculate neurons in terms of cells or neurons/degree^2. This was necessary because in order to obtain convergence ratios by dividing density values, the total measure of "area" in each structure needs to be equivalent, e.g. the retina and geniculate have different total area values when expressed in mm^2, but the same when expressed in degrees^2. This was done by determining an area-metric magnification factor (MF) for each structure, which

specifics the amount of area (in mm^2) in each structure dedicated to a given amount of visual field (in $degrees^2$) [and then multiplying the MFs by the cell densities (in $cells/mm^2$) to get $cells/degree^2$]. The surface areas of the retina (approximately 196 mm^2, from Peterson & Ulinski, 1979) and the external face of the geniculate complex (approximately 1.10 mm^2) were divided by the total span of the visual field in $degrees^2$ using estimates of the extent of the visual field obtained by Northmore & Granda (1991): $(180\ degrees)^2 = 32{,}400\ degrees^2$. This resulted in a MF in units of $mm^2/degree^2$ of visual space for each structure. The MFs were $6.05 \times 10^{-3}\ mm^2/degree^2$ for the retina and $3.39 \times 10^{-5}\ mm^2/degree^2$ for the geniculate. We assumed that the geniculate receives a complete map of visual space from the retinal surface. These magnification factors could then be used to express the densities of ganglion cells and geniculate neurons in units of $cells/degrees^2$.

The second step was to express distance along horizontal and vertical transects across the retina and geniculate complex in terms of degrees of visual space, instead of millimeters. Distance along retinal transects were calculated using the linear components of the retinal MF: 77 $\mu m/degree$ in both the horizontal and vertical axes (Peterson & Ulinski, 1979). Ganglion cell density ranges from 5 to 130 $cells/degree^2$ (Fig. 7A). A major peak occurs at 0° retinal eccentricity and a minor peak occurs at $-35°$. Plotting cell density along the geniculate transects requires information about the MF at each point in the retinogeniculate map. Since the retinogeniculate map has not been established with physiological techniques, we plotted geniculate neuron density as a function of retinal eccentricity under three different assumptions [by adjusting the horizontal component of the geniculate MF] about the structure of the retinogeniculate projection. We first assumed no regional variation in MF (Fig. 7B). Geniculate neuron

density then ranges from 0.1 – 1.8 cells/degree^2. Peaks in geniculate neuron density occur at eccentricities of –50° and –12°. Cell density levels off to about 0.5 cells/degree^2 at an eccentricity of +20°. Second, we assumed adjusted the horizontal component of the geniculate MF such that the central area of peak ganglion cell density (0 degrees eccentricity) projects to the central area of geniculate neuron density (-12 degrees, Fig. 7 transect B). Third, we assumed [adjusted the horizontal component of the geniculate MF such] that the central area of peak ganglion cell density projects to the central area of peak geniculate neuron density and the minor peak ganglion cell density (–35°) projects to the rostral area of peak geniculate neuron density (-50° on Fig. 6, transect B). Since the MF determines the number neurons dedicated to a given region of visual space, the density of geniculate neurons/unit area of retinal surface (in degrees^2) changes in proportion to the change in MF. Thus, the density values in transects C and D were changed in direct proportion to the changes in MF. Plots 7B,C and D suggest that the shape of the cell density versus eccentricity plot does not depend strongly on the detailed structure of the retinogeniculate map.

Place Figure 7 here

In the final step, convergence ratios, in units of ganglion cells/geniculate neuron, were obtained by dividing ganglion cell density in cells/degrees^2 by geniculate neuron density in cells/degrees^2 at each point along the horizontal meridian. Assuming constant MF (Fig. 8A), the convergence ratio ranges from 15 - 180 ganglion cells/geniculate neuron with a mean of 69 ± 44 ganglion cells/geniculate neuron. The ratio is constant at approximately 40 from the nasal edge of the map to an eccentricity of

about – 10°, where it increases. It ranges from 80 to 110 in the central retinal (around 0°), increases to a peak value of 180 at +20°, and then drops to 30 at 75°. Assuming that the peak area of ganglion cell density projects to the area of peak geniculate neuron density did not significantly change the shape of the convergence ratio curve (Fig. 8B). Nasal eccentricity remained relatively unchanged, but the temporal area of peak convergence (0° to 50°) showed an overall reduction of about 25% and the mean convergence ratio dropped 12% to 61 ± 27 ganglion cells/geniculate neuron. Assuming that both retinal peak density areas project to the two peaks of geniculate peak density resulted in a convergence ratio curve (fig. 8C) that was similar to the curve generated by aligning only the central peak density regions. The mean ± SEM was 63 ± 27 ganglion cells/ geniculate neuron.

Place Figure 8 Here

Figures 9 and 10 illustrate a comparable analysis for vertical transects. Figure 9A the density of ganglion cells along the central vertical transect of the retina. Ganglion cell density ranges from approximately 5 to 130 cells degree^2. A peak occurs at a retinal elevation of about 0°. Ganglion cell density increases more gradually along the ventral slope than it does along the dorsal slope. Figure 9B shows the density of geniculate neurons along a vertical transect through the geniculate map at 0° eccentricity assuming constant MF. Geniculate neuron density ranges from 0.4 – 1.3 cells/degree^2, but remains at a relatively constant density of 1 cell/ degree^2 along most of the transect. Figure 9C shows the neuronal density along a vertical transect through the geniculate map at 0° eccentricity assuming that both ganglion cell density peaks project to the two areas of geniculate neuron peak density. Cell densities for this transect range from 0.2

to 1.9 cells/degree^2, which gently peaks at approximately –10° elevation. Figure 10 shows the convergence ratio of ganglion cells/geniculate neuron for the two transects. Figure 10A plots the convergence ratios for the center transect (Fig. 9B); they range from 8 - 110 ganglion cells/geniculate neuron with a mean of 29 ± 24 ganglion cells/geniculate neuron. Figure 10B plots the convergence ratios for the more nasal transect (Fig. 9C), which range from 4 to 86 ganglion cells/geniculate neurons with a mean of 21 ± 19 ganglion cells/geniculate neuron. The spatial variation in convergence ratio is, again, relatively insensitive to assumptions about the structure of the retinogeniculate map.

Place Figures 9 and 10 Here

This analysis indicates that the convergence ratio of ganglion cells/geniculate neuron is, on average, in the range of 10 - 70 ganglion cells/geniculate neuron. The ratio varies significantly at different points in the retinogeniculate map, being relatively low in the representation of the peripheral retina and relatively high in the representation of the visual streak and retinal peak density areas.

Discussion

Potential Errors

Double counting neurons that are split into adjacent sections can lead to an over estimation of neuron populations (Konigsmark, 1970). Several methods can be used to

compensate for double counting. One is to count neurons in every other section and then determine the number of neurons in skipped slides by taking the average of its preceding and succeeding slides. In this way, cells split into adjacent sections are only counted once. We did not employ this method because the geniculates were divided in a relatively small number of coronal sections (~30 sections for Geniculates 1 and 3) and in many cases, the density varied considerably from slide to slide. Thus, interpolatin cell numbers risked making significant errors. Another method that significantly reduces the double counting error is to count only neuronal nucleoli. Because nucleoli are much smaller than somata or nuclei, there is a smaller chance of them being split into adjacent sections and nucleoli that are split into adjacent sections are much less visible than split somata or nuclei. For instance, it has been shown that only 1.3 to 2.8% of nucleoli are displace in sectioned tissue (Konigsmark, 1970). This method was impractical for our study because the borders of the geniculate complex are fairly ambiguous and are not readily discernable at the higher magnification needed to clearly see nucleoli. Given these drawbacks, we decided that the best approach would be to count neuronal nuclei in every section, and then apply the Abercrombie correction factor as explained in the methods.

Tissue shrinkage caused by histological preparation can range from 30% to 50% and can cause an overestimation of cell densities (Konigsmark, 19). The cell density figures in this study were not corrected for tissue shrinkage. Since the geniculate neuron density values in this study are given in cells/area (mm^2), a 30% to 50% linear shrinkage would overestimate cell densities by a factor of two to four. Shrinkage, however, does not affect the total cell counts or density in cells/$degree^2$.

Geniculate neuron Numbers and Densities

Turtles have approximately 11,000 to 18,000 total geniculate neurons, which is relatively low compared to other vertebrates with well-studied visual systems (Fig. 11), e.g. cats have approximately 360,000 geniculate neurons (Peters & Payne, 1993; Bishop et al., 1953) and monkeys have 1.23 – 2.59 million (Clark, 1941; Weber et al., 2000; Blasco et al., 1999), but is similar to rats which have approximately 18,000 (Satorre & Reinoso-Suarez, 1985).

Place Figure 11 Here

In order to compare the spatial distribution of geniculate neurons to the spatial distribution of retinal ganglion cells, we expressed geniculate neuron density in terms of neurons/area by ignoring the geniculate's mediolateral dimension. However most data on geniculate neuron density in the literature are expressed in terms of neurons/volume. The average shrink-corrected mediolateral width of the turtle geniculate is 0.4 mm (Rainey & Ulinski, 1986), which makes the volumetric estimations of geniculate neuron density vary from 25,000 to 150,000 cells/mm^3 with a mean of 48,000 cells/mm^3. This is considerably higher than geniculate neuron densities of cats (1600 to 53,000 cells/mm^3, Mardarasz et al., 1978), monkeys (14,000 to 60,000 cells/mm^3, Clark et al., 1941; Ahmad & Spear, 1993; Blasco et al., 1999) and rats (14,090 to 16,600 cells/mm^3, Satorre & Reinoso-Suarez, 1985), but is comparable to ferrets (~100,000 cells/mm^3 Williams & Jeffery, 2001).

Convergence and Coverage

We estimated the total mean convergence of retinal ganglion cells/geniculate neuron to be approximately 27:1. This is quite different of cat and monkey retinogeniculate projections where their convergence is approximately 1.0 (Sanderson, 1971; Hughes, 1975; Stone, 1978; Hughes, 1981; Bishop et al., 1953; Peters & Payne, 1993; Perry et al., 1984; Clark, 1941; Weber et al., 2000; Blasco et al., 1999), but is roughly comparable to the situation in rats, which have about 113,000 ganglion cells (Potts et al., 1982) and 18,000 geniculate neurons (Satorre & Reinoso-Suarez, 1985) for a convergence ratio of 6.2.

It is likely that ganglion cell to geniculate neuron convergence ratio varies considerably with eccentricity. Given that the retinogeniculate map has not been determined in detail, we were only able to make rough estimates of this variation. The more central regions of the turtle visual field, i.e. the visual streak area, appears to have larger convergence than more peripheral regions. For instance, the mean convergence calculated for the horizontal meridian of visual space is 60 to 70 (depending on the assumptions made about the retinogeniculate map), which is more than three times the average convergence of the retina and geniculate used in this comparison.[2] The higher convergence ratios of ganglion cells to geniculate neurons in the more central regions of the turtle visual field seems to be consistent with the finding of Peterson & Ulinski (1979) that the convergence ratio of photoreceptors to ganglion cells is higher within the turtle visual streak than in the periphery.

The amount of coverage and overlap in the geniculate is determined by cell density and dendritic field size. As shown above, turtle geniculate neurons have high

density and also they have relatively large dendritic fields (Rainey & Ulinski, 1986), which results in a large amount of overlap, expressed in term of coverage factor (table 2) explained in the results. Such extensive dendritic field overlap implies that in addition to a relatively large convergence of ganglion cells to geniculate neuron it is possible that there is also a considerable divergence in the number of geniculate neurons contacted by any given ganglion cell.

References

Ahmad, A. & Spear, P.D. (1993). Effects of aging on the size, density, and number of rhesus monkey lateral geniculate neurons. *Journal of Comparative Neurology* 33, 631-643.

Belekhova, M.V., Kosareva, A.A., Veselkin, N.P. & Ermakova, T.V. (1979). Telencephalic afferent connections in the turtle *Emys orbicularis*: A peroxidase study. *Journal of Evolutionary Biochemical Physiology* 15, 97-103.

Bishop, P.O., Jeremy, D. & McLeod, J.G. (1953). The phenomenon of repetitive firing n the lateral geniculate nucleus of the cat. *Journal of Neurophysiology* 16, 437-447.

Blasco, B., Avendano, C. & Cavada, C. (1999). A stereological analysis of the lateral geniculate nucleus in adult *Macaca nemestrina* monkeys. *Visual Neuroscience* 16, 933-941.

Clark, W.E. Le Gros (1941). The laminar organization and cell content of the lateral geinculate body in the monkey. *Journal of Anatomy* 75, 419-433.

Dreher, B., Sefton A.J., Ni, S.Y. & Nisbett, G. (1985) The morphology, number, distribution and central projections of Class I retinal ganglion cells in albino and

hooded rats. *Brain Behavior and Evolution* 26(1), 10-48.

Hall, W.C. & Ebner, F.F. (1970). Thalmotelencephalic projections in the turtle (*Pseudemys scripta*). *Brain, Behavior, and Evolution* 3, 135-154.

Hall, J.A., Foster, R.E., Ebner, F.F. & Hall, W.C. (1977). Visual cortex in a reptile, the turtle (*Pseudemys scripta* and *Chrysemys picta*). *Brain Research* 130, 197-216.

Hughes, A. (1975). A quantitative analysis of the cat retinal ganglion cell Topography. *Journal of Comparative Neurology* 163, 107-128.

Hughes, A. (1981). Population magnitudes and distribution of the major modal classes of cat retinal ganglion cell as estimated from HRP filling and a systematic survey of the soma diameter spectra for classical neurones. . *Journal of Comparative Neurology* 197, 303-339.

Illing, R.B. & Wassle H. (1981) The retinal projection to the thalamus in the cat: a quantitative investigation and a comparison with the retinotectal pathway. *Journal of Comparative Neurology* 202(2), 265-85.

Konigsmark, B.W. (19 70). Methods for the counting of neurons. In *Contemporary Research Methods in Neuroanatomy*. ed. Nauta, W.J.H. & Ebbesson, S.O.E. Berlin: Springer-Verlag New York.

Lythgoe, J.N. (1979). *The Ecology of Vision.* Oxford:Clarendon Press.

Madarasz M, Gerle J., Hajdu F., Somogyi, G. & Tombol T. (1978). Quantitative histological studies on the lateral geniculate nucleus in the cat. II. Cell numbers and densities in the several layers. *Journal f ür Hirnforsch* 19(2), 159-164.

Martin, P.R. (1986). The projection of different retinal ganglion cell classes to the dorsal lateral geniculate nucleus in the hooded rat. *Experimental Brain Research* 62, 77-88.

Northmore, D.P.M. & Granda, A.M. (1991). Ocular dimensions and schematic eyes of freshwater and sea turtles. *Visual Neuroscience* 7, 627-635.

Ouimet, C.C., Patrick, R.L. & Ebner, F.F. (1985) The projection of three extrathalamic cell groups to the cerebral cortex of the turtle *Pseudemys. Journal of Comparative Neurology* 237, 77-84.

Perry, V.H., Oehler, R. & Cowey, A. (1984). Retinal ganglion cells that project to the dorsal lateral geniculate nucleus in the macaque monkey. *Neuroscience* 12, 1101 -1123.

Peters, A. & Payne, B.R. (1993). Numerical relationships between geniculocortical afferents and pyramidal cell modules in cat primary visual cortex. *Cerebral Cortex*, 3, 69-78.

Peterson, E.H. (1992). Retinal Structure. In *Biology of Reptilia. Vol. 17, Neurology C. Sensorimotor Integration*, ed. Gans, C & Ulinski, P.S. Chicago: The University of Chicago Press.

Peterson, E.H. & Ulinski, P.S. (1979). Quantitative studies of retinal ganglion cells in a turtle *Pseudemys scripta elegans*. *Journal of Comparative Neurology* 186, 17-42.

Potts, A.M., Hodges, D., Shelman C.B., Frity, K.J., Levy N.S. & Magnall Y. (1972). Morphology of the Primate Optic Nerve. 1. Method and total fibre count. *Investigative Opthalmology & Visual Science* 11, 981-988.

Rainey, W.T. & Ulinski, P.S. (1986). Morphology of neurons in the dorsal lateral geniculate complex in turtles of the genera *Psuedemys* and *Chrysemys*. *Journal of Comparative Neurology* 253, 440-465.

Rodieck,…

Sanderson , K.J. (1971). Visual field projection columns and magnification factors in the lateral geniculate nucleus of the cat. *Experimental Brain Research* 13,159-177.

Satorre, J., Cano, J. & Reinoso-Suarez, F. (1985). Stability of the neuronal population of the dorsal lateral geniculate nucleus (LGNd) of aged rats. *Brain Research* 339, 375-

77.

Schein, S.J. & Monasterio, F.M. (1987). Mapping of retinal and geniculate neurons onto striate cortex of macaque. *The Journal of Neuroscience* 7(4), 996-1009.

Sterling, P. (1998) Retina. In *The Synaptic Organization of the Brain 4th ed.*, ed. Shepherd, G.,

New York: Oxford University Press.

Stone, J. (1978). The number and distribution of ganglion cells in the cat's retina. *Journal of Comparative Neurology* 180, 753-771.

Ulinski, P.S. (1999). Neural mechanisms underlying the analysis of moving visual stimuli. In *Cerebral Cortex. Vol. 13. Models of Cortical Circuitry,* ed. Ulinski, P.S. & Jones, E.G., New York: Plenum Press.

Ulinski, P.S. & Nautiyal, J. (1988). Organization of retinogeniculate projections in turtles of the genera *Pseudemys* and *Chrysemys*. *Journal of Comparative Neurology* 276, 92-112.

Weber, A.J., Chen, H., Hubbard, W.C. & Kaufman, P.L. (2000). Experimental glaucoma and cell Size, density, and number in the primate lateral geniculate nucleus. *Investigative Opthalmology & Visual Science* 41(6), 1370-1379.

Williams, A.L. & Jeffery, G. (2001). Growth dynamics of the developing lateral geniculate nucleus. *Journal of Comparative Neurology* 430, 332-342

Woodbury P.B. & Ulinski P.S. (1986). Conduction velocity, size and distribution of optic nerve axons in the turtle, *Pseudemys scripta elegans*. *Anat Embryol* 174(2), 253-63.

Figure Legends

Figure 1. **A**. Depicts the retino-geniculate projection (adapted from Peterson & Ulinski, 1979). The nasotemporal axis is mapped along the rostrocaudal axis of the contra lateral geniculate. A small ipsilateral projection indicated by crosshatched area extends along the ventral crescent of the retina and the ventral half of the geniculate. **B**. Shows a *camera lucida* drawing of Geniculate-2 in transverse section at approximately the position indicated in A. Neuropile (NP) and cellplate (CP) components of the geniculate are as indicated. Each section was divided into rows with heights of 50 μm. **C**. Displays a 3-D rendition of B. The mediolateral distribution of neurons was ignored and all cells within each rectangular solid were counted as if they occurred on the geniculate's lateral face (in the rostrocaudal, dorsoventral plane).

Figure 2. Isodensity contour maps of geniculate neurons for Geniculate - 1. These maps show the spatial distribution of geniculate neurons for the geniculate's two cell types (the neuropile and cell plate) and for all cells. Contour line numbers correspond to units of thousands of cells/mm^2. Note the two areas of peak cell density, one positioned ventrally in approximately the center of the rostrocaudal axis and one slightly more dorsal and rostral.

Figure 3. Isodensity contour maps of geniculate neurons for Geniculate - 2. These maps show the spatial distribution of geniculate neurons for the geniculate's two cell types (the neuropile and cell plate) and for all cells. Contour line numbers correspond to units of thousands of cells/mm^2. Note the two areas of peak cell density, one positioned ventrally in approximately the center of the rostrocaudal axis and one slightly more dorsal and rostral.

Figure 4. Isodensity contour maps of geniculate neurons for Geniculate - 3. These maps show the spatial distribution of geniculate neurons for the geniculate's two cell types (the neuropile and cell plate) and for all cells. Contour line numbers correspond to units of thousands of cells/mm^2. Note the two areas of peak cell density, one positioned ventrally in approximately the center of the rostrocaudal axis and one slightly more dorsal and rostral.

Figure 5. Plots of cell density along rostrocaudal transects for Geniculate – 2. The position of each transect is indicated on the inset. The dorsal-ventral (D-V) and rostral-caudal (R-C) axes are indicated for the inset. Transects C & D passes through both of the geniculate's areas of peak density. Transect C used in Figure 7 to compare the geniculate's cell distribution to retinal ganglion cell distribution.

Figure 6. Plots of cell density along dorsoventral transects for Geniculate – 2. The position of each transect is indicated on the inset. The dorsal-ventral (D-V) and rostral-caudal (R-C) axes are indicated for the inset. Transect D passes through the more central area of peak cell density and is used in Figure 8 to compare the geniculate's cell distribution to retinal ganglion cell distribution.

Figure 7. **A**. Plot of ganglion cell density along the horizontal meridian of the retina (adapted from Peterson & Ulinski, 1979). **B**. Plot of geniculate neuron density along the horizontal meridian of the geniculate, assuming a constant magnification factor (MF) of 3.39×10^{-5} mm^2/deg^2. **C.** Plot of transect B with the MF varied such that the central area of peak ganglion cell density (0 degrees, transect A) aligns with the more central area of peak geniculate neuron density (-12 degrees, transect B). To align these peak areas, the

MF of the nasal region of transect B (-88 to –12 degrees) was decreased by a factor of 0.86 (MF = 2.92 x 10^{-5} mm^2/deg^2), and the MF of the temporal region of transect B (-12 to 90 degrees) was increased by a factor of 1.14 (MF = 3.86 x 10^{-5} mm^2/deg^2). **D.** Plot of transect B with MF varied such that the central areas of ganglion and geniculate neuron density align (as in transect C) and such that the nasal area of peak geniculate density of transect B (-50 degrees) aligns with the more nasal area of minor ganglion cell peak density (-35 degrees, transect A). To align these peak areas the MF of transect B was varied as follows: -88 to –50 degrees decreased by a factor of 0.70 (MF = 2.37 x 10^{-5} mm^2/deg^2), -50 to –12 degrees increased by a factor of 1.07 (MF = 3.63 x 10^{-5} mm^2/deg^2), and –12 to 90 degrees increased by a factor of 1.14 (MF = 3.86 x 10^{-5} mm^2/deg^2). The relative cell density values of transects C & D were changed in direct proportion to a change in MF.

Figure 8. Plots of ganglion cells/geniculate neuron convergence ratios obtained by dividing ganglion cell density values (Fig. 7A) by geniculate neuron density values (Fig. 7B, C, & D) at corresponding points of retinal eccentricity. **A.** Shows the convergence ratios using a constant magnification factor (MF) geniculate transect (Fig. 7B). The mean convergence for this graph is 69 ± 44 ganglion cells/geniculate neuron. **B.** Shows the convergence ratios using the varied MF scheme of Fig. 7C, and has a mean convergence of 61 ± 27 ganglion cells/geniculate neuron. **C.** Shows the convergence ratios using the varied MF scheme of Fig. 7D, and has a mean convergence of 63 ± 27 ganglion cells/geniculate neuron.

Figure 9. Comparison of ganglion cell and geniculate neuron densities, plotted as vertical transects at the positions indicated on the insets. **A.** Shows the retinal transect

that passes through the area of peak ganglion cell density (adapted from Peterson & Ulinski, '79). **B.** Shows the geniculate transect that intersects the constant magnification, center, horizontal transect (Fig. 7B) at 0° eccentricity. **C.** Shows the geniculate transect that intersects the varied magnification, center, horizontal transects (Fig. 7D,C) at 0° eccentricity. The magnification factor (MF) for the geniculate transects is constant (MF = 3.39×10^{-5} mm^2/deg^2).

Figure 10. Plots of ganglion cells/geniculate neuron convergence ratios obtained by dividing ganglion cell density values (Fig. 9A) by geniculate neuron density values (Fig. 9B,C) at corresponding points along retinal elevation. **A**. Shows the convergence ratios using Fig. 9B, and has a mean convergence of 29 ± 24 ganglion cells/geniculate neuron. **B.** Shows the convergence ratios using the lower geniculate transect from Fig. 9, and has a mean convergence of 21 ± 19 ganglion cells/geniculate neuron.

Figure 11. Displays typical literature values of total number of ganglion cells and geniculate neurons for cats, monkeys, rats, and turtles. Cats have approximately 100,000 to 140,000 ganglion cells (Sanderson, 1971; Stone, 1978), 60-77% of which project to the geniculate (Illing & Wässle, 1981;Review: Sterling, 1998), and 450,000 to 560,000 geniculate neurons (Peters & Payne, 1993; Bishop & McLeod, 1953) with approximately 25% of these being interneurons (Peters & Payne, 1993). Monkeys have approximately 1.2 to 1.4 million ganglion cells (Perry et al., 1984), 90% of which project to the geniculate (Perry et al., 1993), and 1.3 to 2.6 million geniculate neurons (Clark, 1941; Connolly & Van Essen, 1984; Blasco et al., 1999; Weber et al., 2000). Rats have 110,000 to 115,000 ganglion cells (Potts et al., 1982; Perry et al., 1983), less than 50% of which project to the geniculate (Dreher et al., 1985; Martin, 1986), and 17,000 to 20,000

geniculate neurons (Satorre & Reinoso-Suárez, 1985). Turtles have 350,000 to 390,000 ganglion cells (Peterson & Ulinski, 1979), ##% of which project to the geniculate ( ), and 11,000 to 18,000 geniculate neurons. Thus, the approximate total ganglion cell/geniculate neuron ratios are as follows, monkeys: 1:1 (Schein & Monasterio, 1987), cats: 1:5 (Sanderson, 1971), rats: 3:1 (calculated using above cited values), and turtles: 27:1 (calculated using above cited values).

Footnotes

1. John's new address
2. Genicualte-2 and Retina M28-R (from Peterson & Ulinski, 1979) were used to estimate the convergence ratios in figures 7-9. Geniculate-2 had a total of 18,122 neurons and M28-R had a total of 362,000 ganglion cells, so the mean convergence ratio for this retina and geniculate is 20:1.

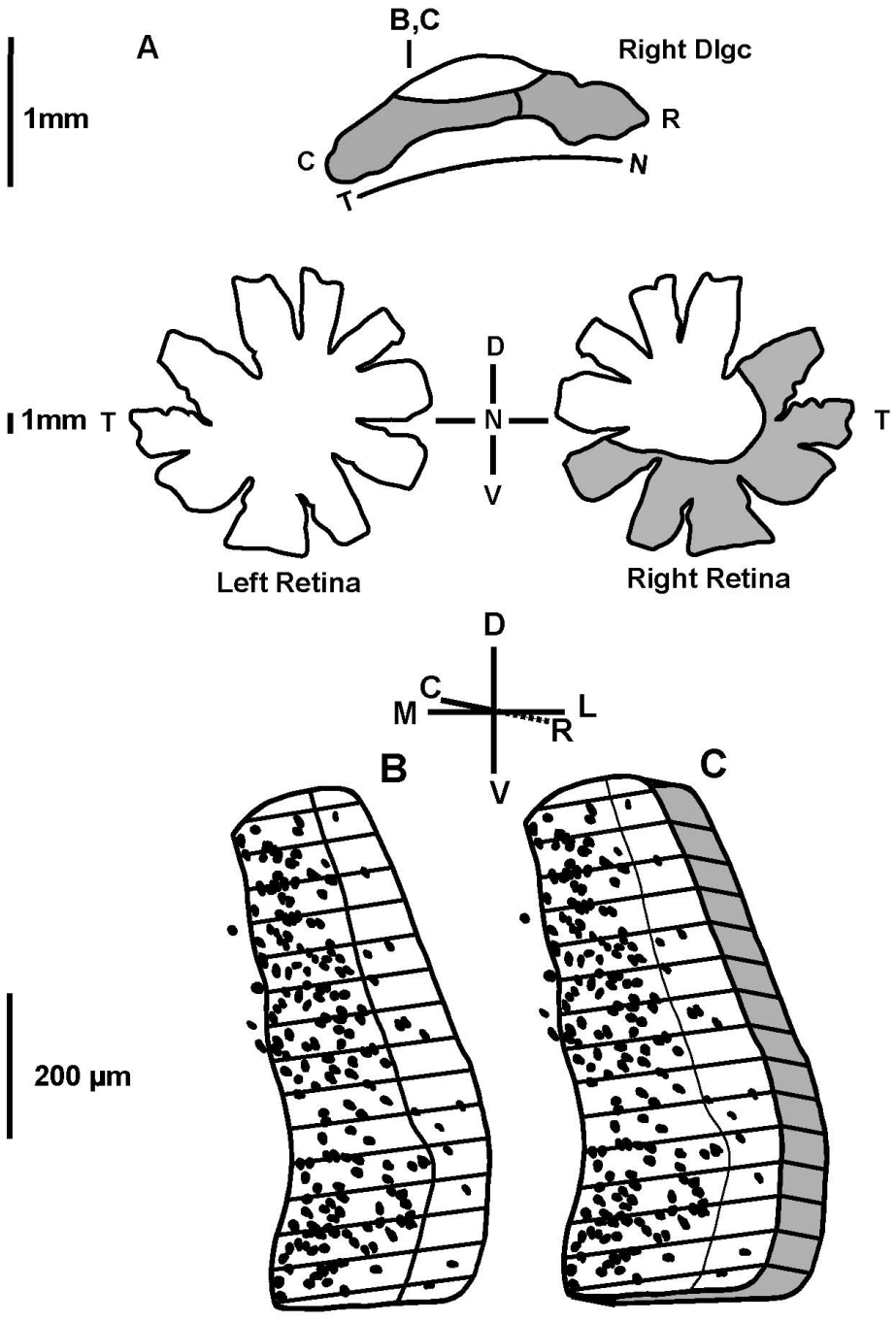
A
B,C
Right Dlgc
1mm
C
R
N
T
1mm
T
D
N
V
T
Left Retina
Right Retina
D
C
M
L
R
V
B
C
200 µm

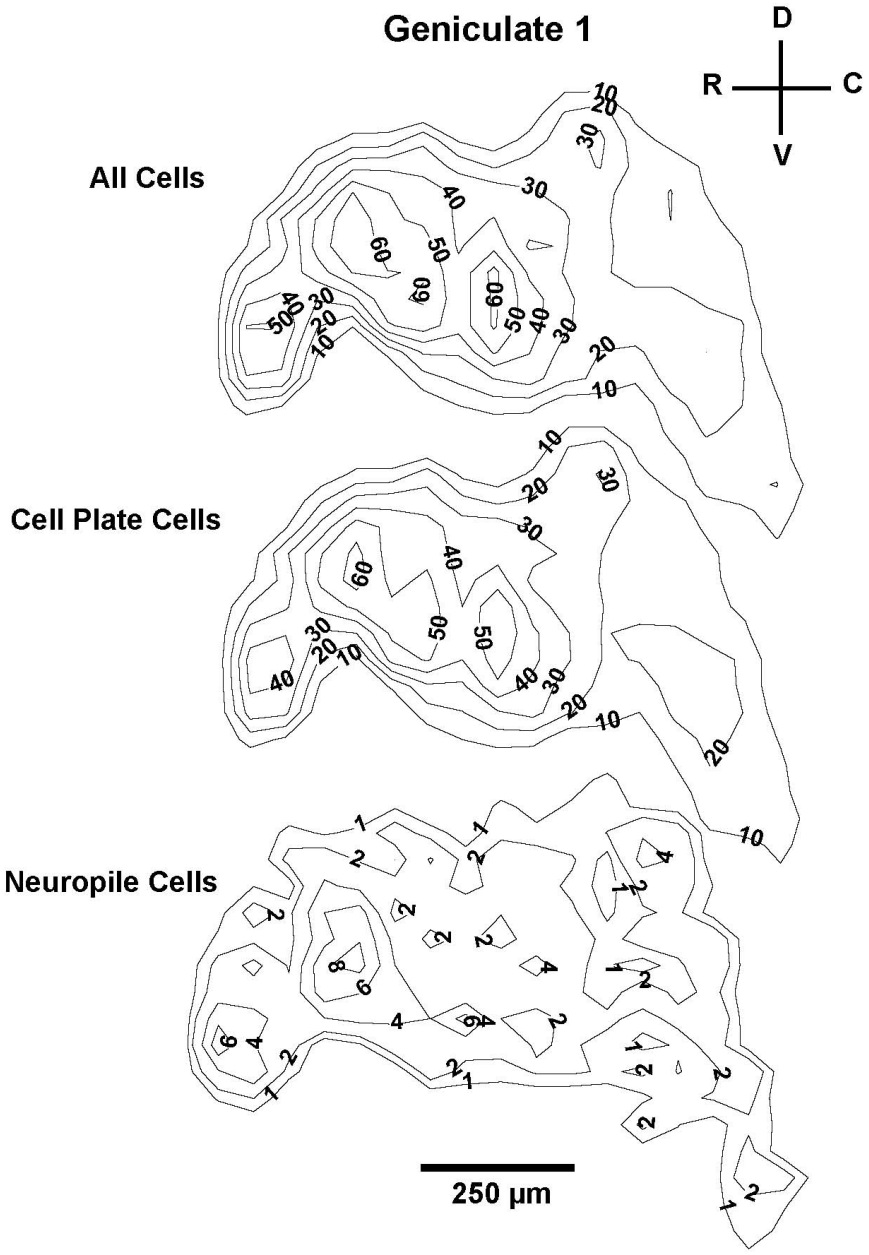
Geniculate 1
D
R
C
V
All Cells
Cell Plate Cells
Neuropile Cells
250 µm

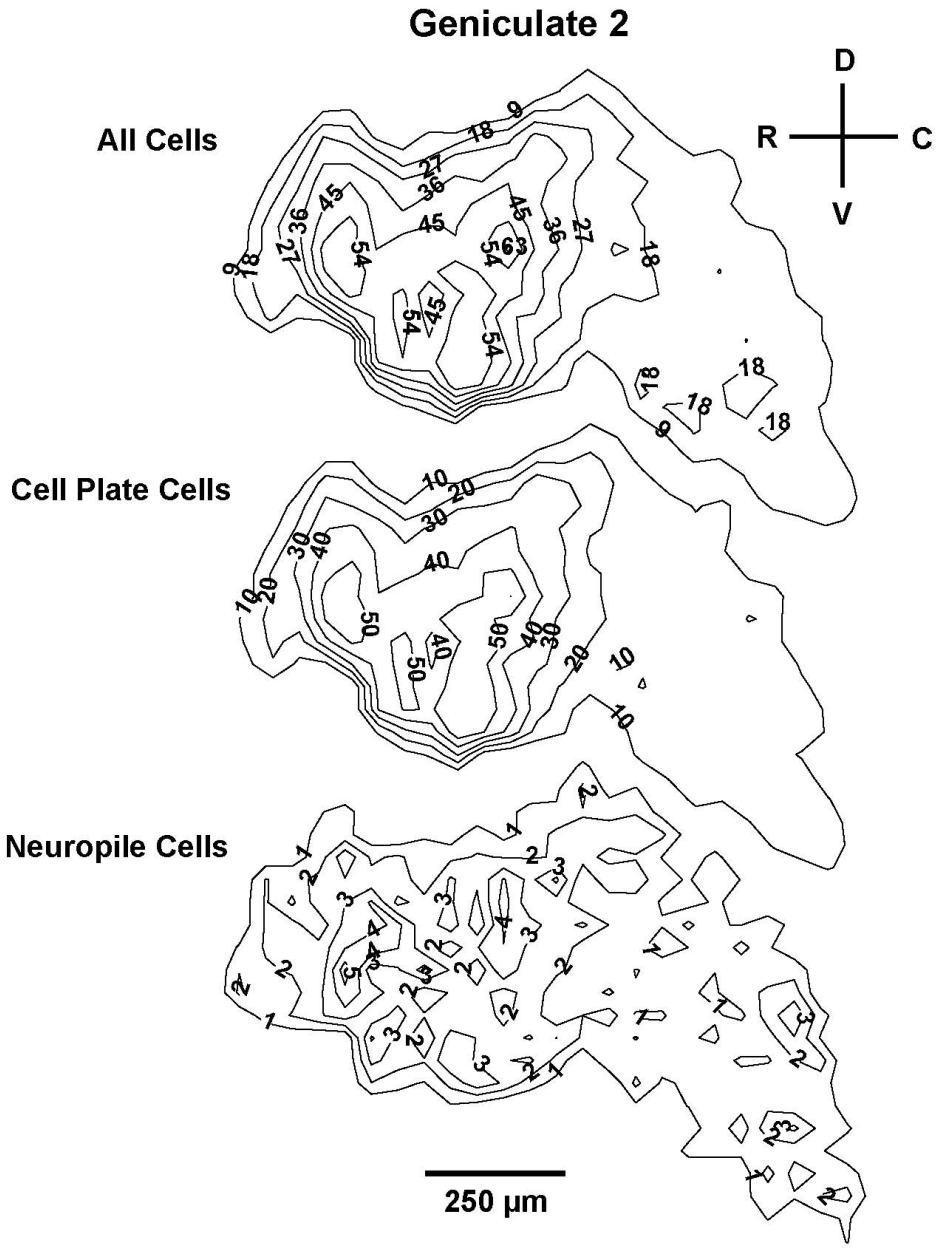
Geniculate 2
All Cells
Cell Plate Cells
Neuropile Cells
D
R
C
V
250 µm

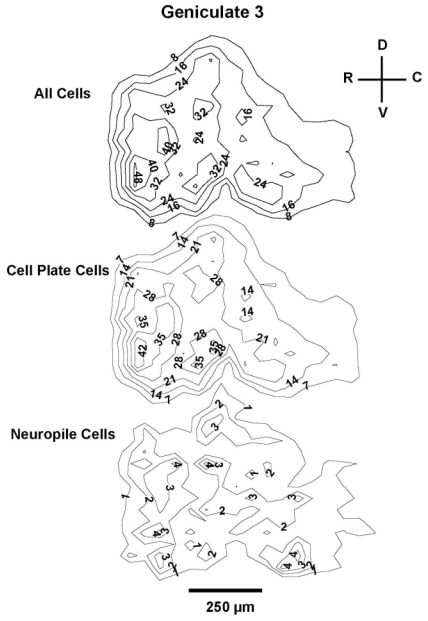
Geniculate 3
All Cells
Cell Plate Cells
Neuropile Cells
D
R
C
V
250 µm

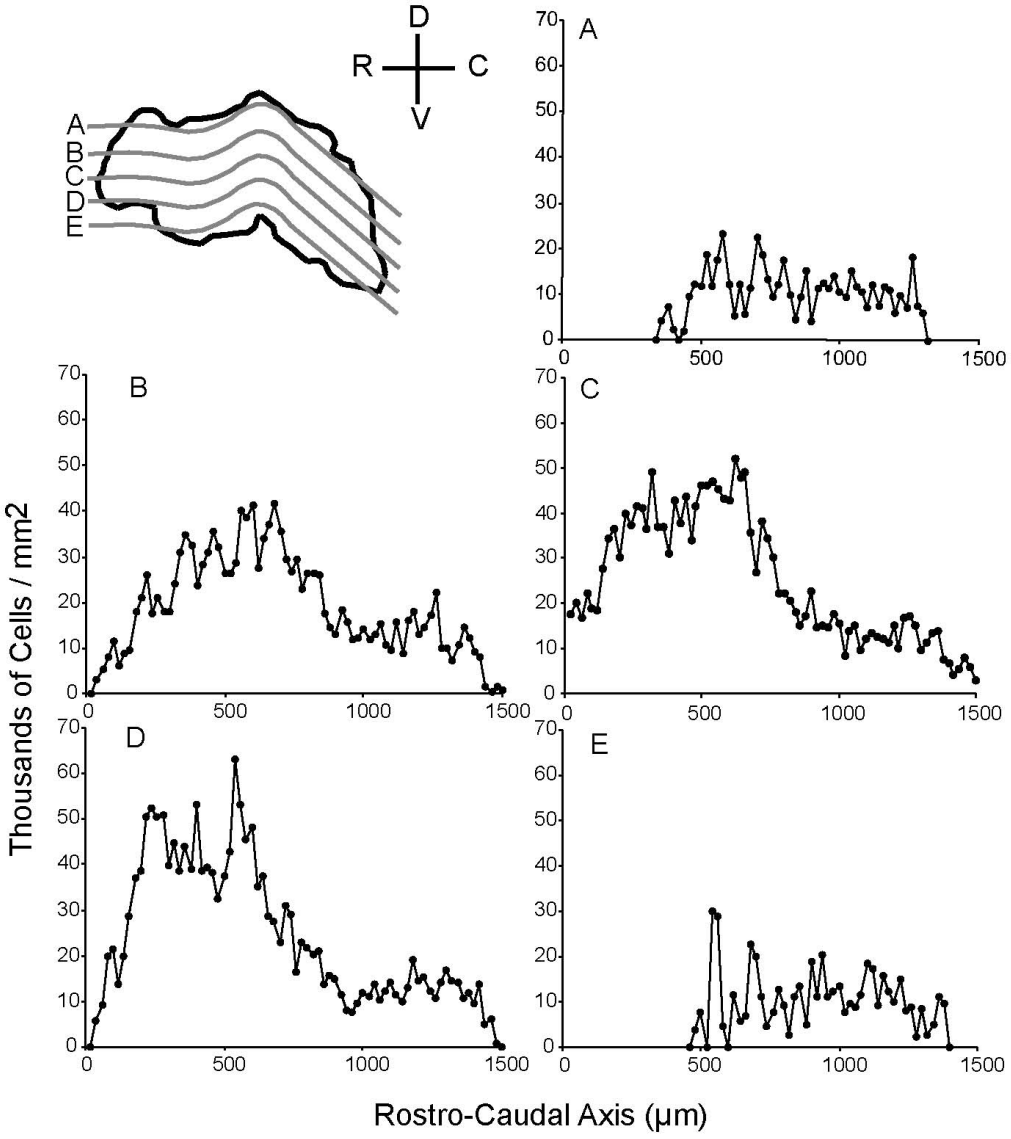
D
R
C
V
A
B
C
D
E
A
B
C
D
E
Thousands of Cells / mm2
Rostro-Caudal Axis (µm)
0
10
20
30
40
50
60
70
500
1000
1500

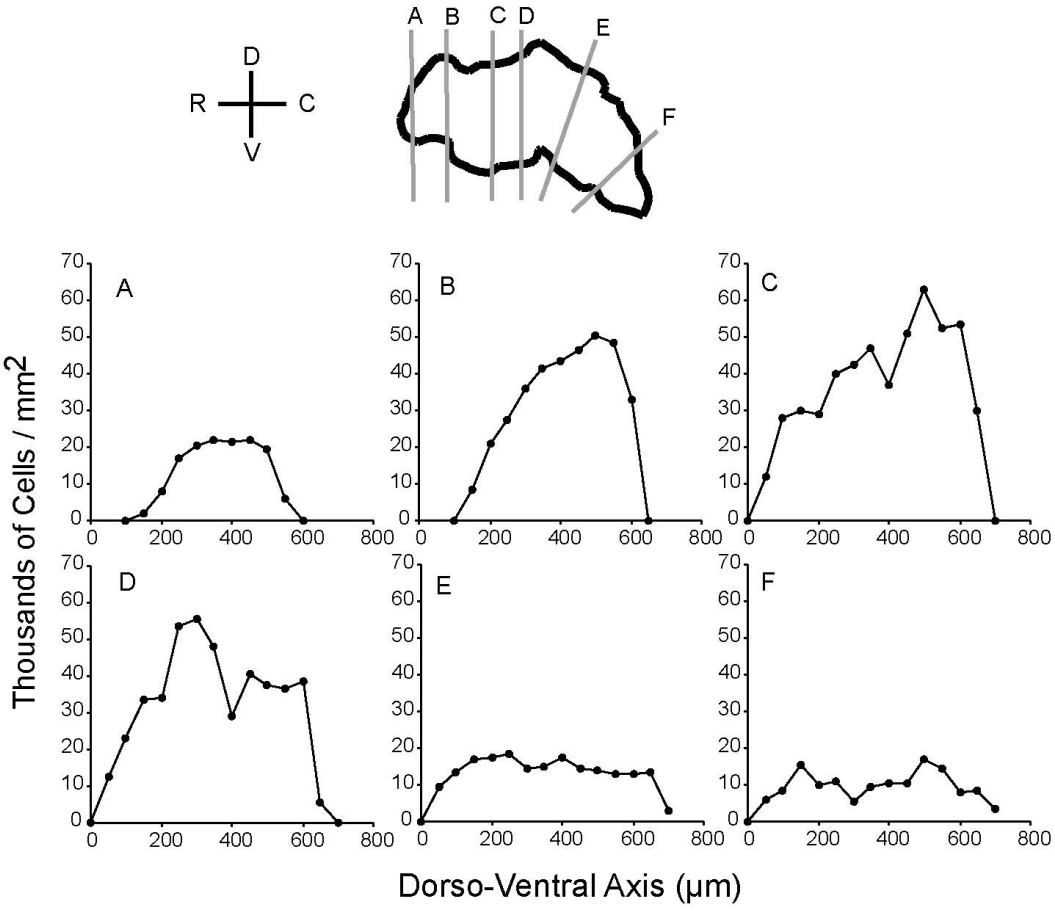
D
R
C
V
A
B
C
D
E
F
A
B
C
D
E
F
Thousands of Cells / mm2
Dorso-Ventral Axis (µm)

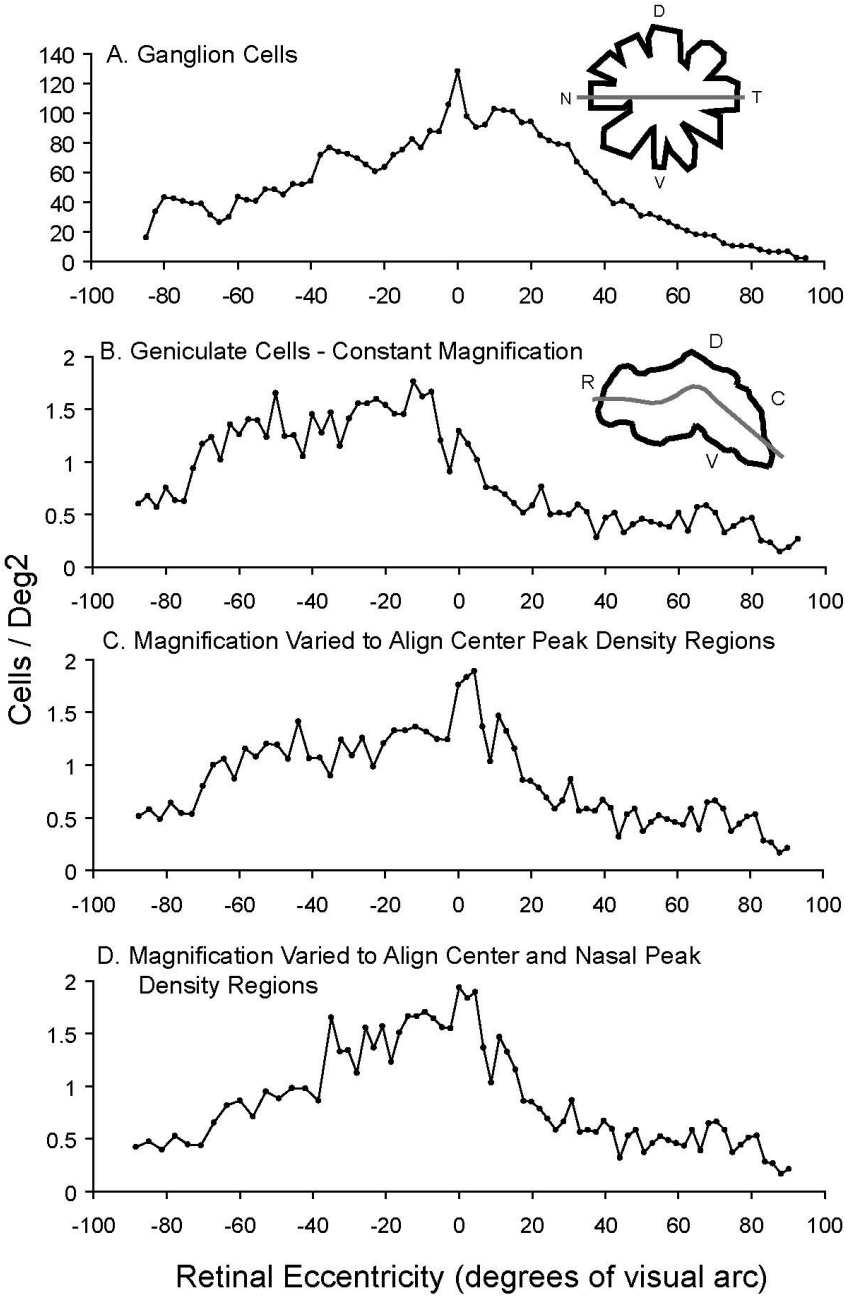
A. Ganglion Cells
D
N
T
V
140
120
100
80
60
40
20
0
-100 -80 -60 -40 -20 0 20 40 60 80 100
B. Geniculate Cells - Constant Magnification
D
R
C
V
2
1.5
1
0.5
0
C. Magnification Varied to Align Center Peak Density Regions
D. Magnification Varied to Align Center and Nasal Peak Density Regions
Cells / Deg2
Retinal Eccentricity (degrees of visual arc)

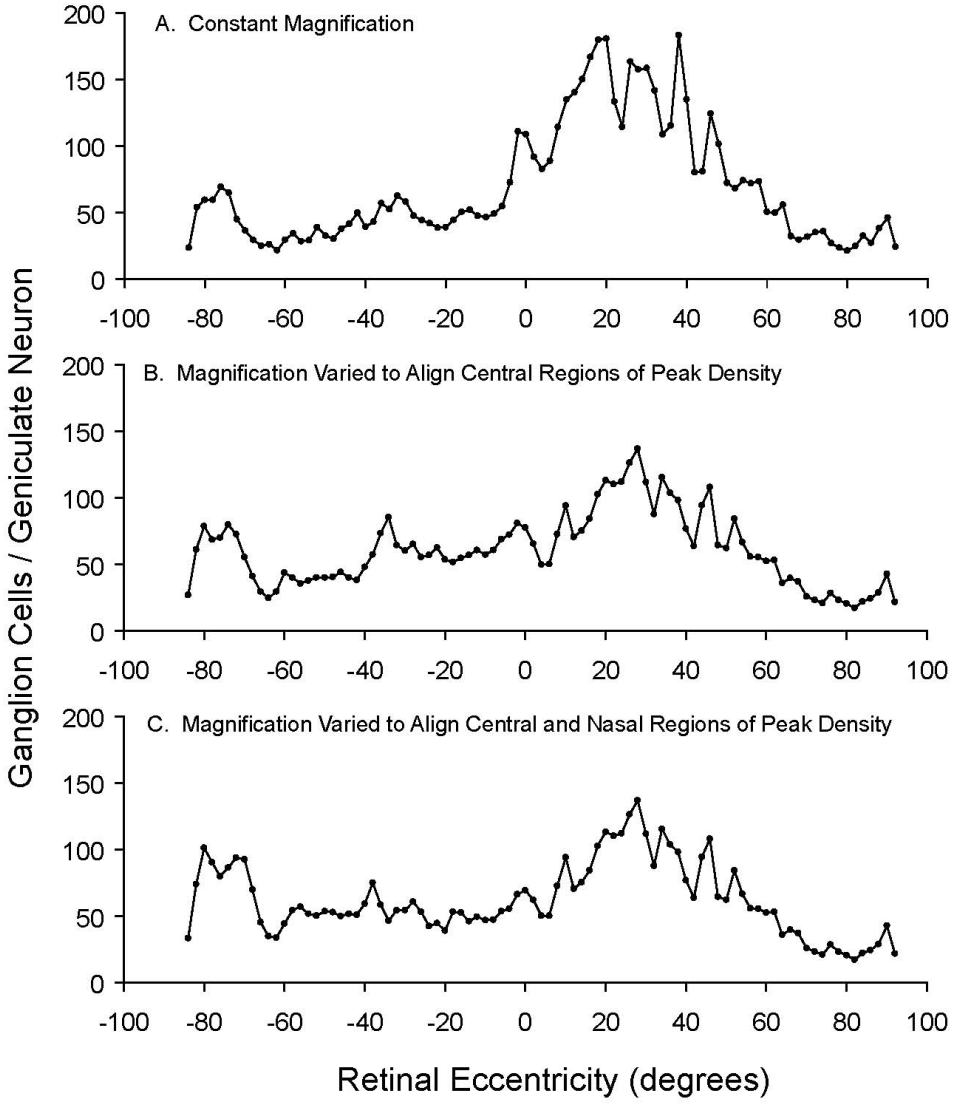
A. Constant Magnification
B. Magnification Varied to Align Central Regions of Peak Density
C. Magnification Varied to Align Central and Nasal Regions of Peak Density
Ganglion Cells / Geniculate Neuron
Retinal Eccentricity (degrees)
200
150
100
50
0
-100
-80
-60
-40
-20
0
20
40
60
80
100